Journal of Sound and Vibration (1997) **201**(1), 103–125

MEASURING THE RELATIVE STRENGTHS OF A SET OF PARTIALLY COHERENT ACOUSTIC SOURCES

M. J. Fisher and K. R. Holland

Institute of Sound and Vibration Research, University of Southampton, Southampton SO17 1BJ, England

(*Received* 28 *May* 1996, *and in final form* 28 *August* 1996)

The measurement of the relative contributions to the acoustic field made by a set of sources, which by necessity must operate simultaneously, is of importance in many areas of noise control technology. A partial solution to this problem, proposed in the 1970s, was the Polar Correlation Technique. This recognized, initially, the Fourier transform relationship between cross-spectra, measured in the acoustic far field, and the distribution of source strength of a line array of sources, typical of an aero-engine, for example. In a second development (1981) a parametric method was developed. Essentially, the position of the contributing sources was assumed to be known and a least squares error procedure was employed to establish an optimum fit between the source strength distribution and the cross-spectral data. A major restriction, however, was the necessary assumption of mutually incoherent sources. In the present work it is demonstrated that this restriction is unnecessary, albeit at the expense of some extra data processing. Specifically, we show that by employing several reference microphones, as opposed to one for incoherent sources, both the amplitude of and coherence between an array of sources may be determined. The potential capability of the method is established both analytically and through extensive numerical simulation.

1. INTRODUCTION

The estimation of the relative contribution to the acoustic field made by a set of sources, which by necessity must operate simultaneously, is important in many areas of noise control technology. Developments in this area during the 1970s, in the context of aircraft noise, led to the development of the Polar Correlation Technique [1]. This recognized the Fourier transform relationship which exists between the source strength distribution of a line source and cross-spectra measured between microphones located on a polar arc in the far field. As originally conceived, the method yielded a resolution limited image of the true source distribution. In a second development, a parametric approach was adopted [2]. Here, briefly, one assumes that the source positions are known and then employs a least squares fit procedure to calculate the set of source strengths which provide minimum error with respect to the measured cross-spectral data. We shall return to the advantages of this class of technique later. However, a major restriction of the techniques described in references [1] and [2] was the requirement that all sources had to be mutually incoherent. In this paper it is demonstrated how the basic method may be generalized to include an array of partially coherent sources; albeit at the price of extra data processing. Specifically, it will be shown that, while for incoherent sources measurement of the cross-spectra

0022–460X/97/110103 + 23 $25.00/0/sv960743

between one reference microphone and others in the array is sufficient, for coherent sources a number of such reference microphones must be employed.

In the interests of brevity, we shall explore the capabilities and limitations of this method in terms of a line array of partially coherent monopoles, the phasing of which is set by a disturbance convecting through them, as shown in Figure 1. The astute reader will note a marked similarity with the shock associated noise model first proposed in reference [3] and, indeed, this was the original motivation for the work. However, as will be shown, the method is perfectly general and can be applied to any source–microphone arrangement. The principal advantage of the line source configuration in the present context is that it permits certain analytical results to be obtained which provide a degree of understanding not available from numerical simulation alone.

1.1. BACKGROUND

While the class of techniques discussed in this paper are frequently referred to as "Source Location Methods", this is to some extent a misnomer. The objectives of source location, in the context of sonar for example, is the detection of a source of unknown location and in the presence of significant background noise and other complications. Conversely, for noise control application, the location or vicinity of potentially contributing sources is usually known; the objective is to assess the relative contributions which they make to the total noise field. The application of such data may include the following: identifying that source or subset of sources which require the application of noise control methods before any significant improvement of the noise environment can be anticipated; confirming that these methods have been successful and have not created adverse effects on other sources; and, in a slightly different context, to use such source distributions as the basis for calculation of acoustic pressures in either the geometric near or far field of the source array.

A major incentive for this type of investigation arose in the 1970s and early 1980s in the context of aircraft noise. The applications were twofold. More fundamental was the desire to measure the axial distribution of "source strength" for jet shear flows. However, the advent of the high bypass ratio engines (i.e., the Rolls Royce RB-211) provided a second application; the measurement of the so-called "Engine Noise Source Breakdown" [2]. These are of relevance not only in the noise control sense outlined above, but are also important in the detremination of the static-to-flight noise changes which may be anticipated.

The approaches to "source contribution" determination developed at that time fall naturally into two classes. The first historically, which we believe was originally attributatble to Siddon [4], became known as "Causality Correlation" techniques. These

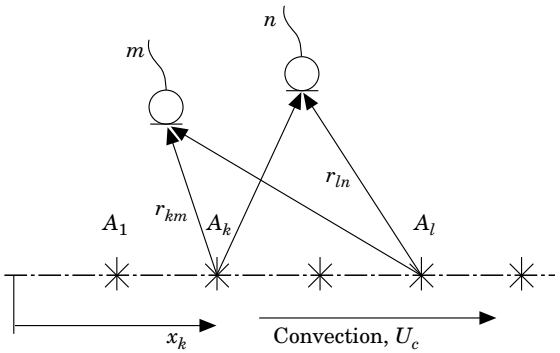

Figure 1. An array of partially coherent monopole sources.

involved the determination of the coherence between an "in-source" probe and a far field microphone as a measure of the fraction of the mean square pressure at the microphone contributed by the "source" under investigation. Such techniques involved a range of practical difficulties and, more fundamentally, a need for a presupposition of the noise producing mechanisms involved, since these determined what should be measured by the source probe.

The second general class of techniques avoided these problems by restricting measurements to the acoustic field alone. They include the parabolic and elliptic mirror measurements of Chu and Laufer [5] and Grosche [6] respectively. While such methods are apparently both simple to apply and effective at model scale, the requirements of adequate resolution and gain lead to prohibitive mirror sizes for full scale aero-engine application. An estimate by Glegg [7] suggests that mirrors of 25 feet diameter might be required in this context. We note further that for the more desirable elliptic mirror the distance between the microphone at one focus and the source at the other is fixed, so that physical traversing of the mirror is required to explore an extended source distribution.

An awareness of these problems led workers in the U.K. to explore the possibility of replacing reflecting surfaces with arrays of microphones. One such system, termed the "Acoustic Telescope", was described by Billingsley and Kinns [8] and comprised a line array of microphones. Beam forming and/or focusing of the array was achieved by introducing time delays into the various microphone channels prior to a summation. A recent survey of this class of technique has been provided by Mosher [9], who notes that the improved performance to cost ratio of electronic equipment and computers makes it increasingly practical to make acoustic measurements with phased arrays containing many microphones. Indeed, it is the number of microphones required in practice which, arguably, sets the limit on all microphone array methods. Even for an assumed line array [8], one needs a sufficient array aperture to resolve at the lowest frequency of interest f_1 the most closely spaced sources at distance l apart, while simultaneously having sufficiently closely spaced microphones to prevent aliasing at the highest frequency of interest f_2 for the entire length of the real source distribution L. This leads to a requirement for N microphones, given by $(N-1) = (L/l)(f_2/f_1)$, a number which can easily reach 100 in practical situations, in which results over perhaps a decade of frequency are required. Furthermore, we note that for the phased array methods all these microphones must be positioned simultaneously.

A method developed concurrently with the "Acoustic Telescope" [8] was the Polar Correlation Technique [1]. This approach recognized a Fourier transform relationship between the cross-spectra measured between microphones in the far field and a distribution of source strength. This type of what might be termed a "statistical" approach has some advantages over phased arrays in terms of both data acquisition and the subsequent data processing.

First, while the number of microphone measurement positions is identical with that required for the phased array approach, all the required cross-spectra could, in principle, be measured with as few as two microphones if facility operating economics so dictate. Even more attractive is the natural "break" in the data processing which occurs once the cross-spectra have been determined. These form a relatively compact data storage bank from which information can be subsequently retrieved for a wide range of post-processing operations. Furthermore, the ability selectively to choose data, for various frequency ranges, can be employed to reduce microphone numbers, as has been reviewed in some detail by Glegg [10], while the possibility of creating "virtual" microphone positions has been discussed by Strange *et al*. [11].

Despite these advantages, it became apparent that for routine source breakdown work the processing of resolution limited source images to obtain the spectrum of individual sources was extremely time consuming and required siginficant judgement as the limits of resolution were approached. An awareness of this problem led to the development of the parametric or source model based approach, first described in reference [2]. In principle, one sets up a model of the source distribution and determines a set of unknown source amplitudes from a least squares fit between the calculated and measured cross-spectra. Practical problems, in particular some uncertainty in source position, can be overcome by iterating these positions across a limited window until the difference between the modelled and measured cross-spectra is minimized in a least squares sense.

However, a major restriction of this class of technique, as described in references [1] and [2] and applied in reference [11], was the inherent assumption that all the contributing sources were mutually incoherent. We note in this context that Mosher [9] comments that "The most difficult situations probably involve distributed coherent sources". The purpose of this paper is to show how this particular problem can be successfully addressed using an extension of the model based approach.

However, in closing this section we note that some formidable problems do remain to be overcome. Not least among these is the question of source directivities. Most of the methods described above implicitly assume that the source array is comprised of incoherent monopoles, despite the fact that the acoustic measurements demonstrate directional characteristics. This is not a serious complication if one can reasonably assume [1] that all sources have similar, strictly identical, directivities at each frequency. It also seems probable, but is currently unproven, that the model based approaches would cope with inherent source directivities if these were known *a priori* and could be included in the source model. However, the determination of unknown source directivities in situations in which sources could be either incoherent or coherent presents a formidable challenge and is perhaps leading towards ambiguous possibilities; an extreme version of which was so elegantly described by Kempton [12]. Certainly, at the present state-of-the-art, it would seem that the more prior knowledge of the source characteristics which can be employed from the outset, the more reliable the results obtained will be.

2. A MODEL

Consider the line source array in Figure 1, for which source fluctuations at sources k and l, respectively, are partially coherent and driven by a convecting disturbance of velocity U_c: i.e., the filtered cross-correlation function is of the form

$$\overline{A_k(t)A_l(t+\tau)} = a_k a_l c_{kl} \exp \mathrm{j}\omega\left(r - \frac{x_l - x_k}{U_c}\right),$$

where a_k is the r.m.s. amplitude and c_{kl} is the correlation coefficient between sources k and l respectively.

The cross-spectrum between microphones m and n can then be written as

$$C(m,n) = \sum_k \sum_l \frac{a_k a_l c_{kl} \exp \mathrm{j}\omega\left[\dfrac{r_{km} - r_{ln}}{a_0} + \dfrac{x_k - x_l}{U_c}\right]}{r_{km} r_{ln}}, \tag{2.1}$$

where r_{km} is the distance from source k to microphone m, r_{ln} is the distance from source l to microphone n and a_0 is the speed of sound. We note here that the phase of the cross-spectrum comprises two terms: $(r_{km} - r_{ln})/a_0$, representing a difference of propagation times; $(x_k - x_l)/U_c$, representing the "phase" difference between sources k and l respectively. Hence equation (2.1) can be generalized to any situation in which the source–microphone geometry and the relative phasing of the sources is known, and rewritten as

$$C(m, n) = \sum_k \sum_l b_{kl} \exp \mathrm{j}\phi(m,n, k, l). \tag{2.2}$$

Therefore, clearly, the task is basically to use a set of cross-spectral measurements $C(m, n)$ in conjunction with known values of $\phi(m, n, k, l)$ to determined the unknown values of b_{kl}. As previously discussed in reference [2], a least squares fit procedure is advantageous in view of the statistical errors inevitably involved in such cross-spectral measurements.

2.1. THE LEAST SQUARES FIT

The objective is to find a set of sources, b_{pq}, having the same positions and phases as those specified in equation (2.2), which will minimize the mean square error between the measured cross-spectra and those calculated from the model equation (2.2). The error to be minimized is defined as

$$\sigma^2 = \frac{1}{M} \sum_m \frac{1}{N} \sum_n |\tilde{C}(m, n) - C(m, n)|^2, \tag{2.3}$$

where $\tilde{C}(m, n)$ denotes the measured values. To find the minimum error then requires that

$$\partial\sigma^2/\partial b_{pq} = 0. \tag{2.4}$$

As shown in the Appendix, insertion of equation (2.2) into equation (2.4) yields

$$\frac{1}{M}\frac{1}{N} \sum_m \sum_n \tilde{R}(m, n) \cos \phi(m, n, p, q) + \tilde{I}(m, n) \sin \phi(m, n, p, q)$$

$$= \sum_k \sum_l b_{kl} \frac{1}{M} \sum_m \frac{1}{N} \sum_n \cos (\phi(m, n, k, l) - \phi(m, n, p, q)), \tag{2.5}$$

where $\tilde{R}(m, n)$ and $\tilde{I}(m, n)$ are the real and imaginary parts of the measured cross-spectra, respectively. It is also shown in the Appendix that equation (2.4) yields a single unique minimum with $\partial^2\sigma^2/\partial b_{pq}^2 = 2$.

Inspection of equation (2.5) shows that the left side is comprised of a set of measurements, combined with some geometric information. For each pair of values (p, q), one can therefore write

$$\underline{M}\tilde{(}p, q) = \sum_k \sum_l b_{kl} \frac{1}{M} \sum_m \frac{1}{N} \sum_n \cos (\phi(m, n, k, l) - \phi(m, n, p, q)), \tag{2.6}$$

where $\tilde{M}(p, q)$ is a vector of measurements of dimension $K^2 \times 1$ for K sources which equates to the product of a vector of source "amplitudes" B, also of dimension $K^2 \times 1$,

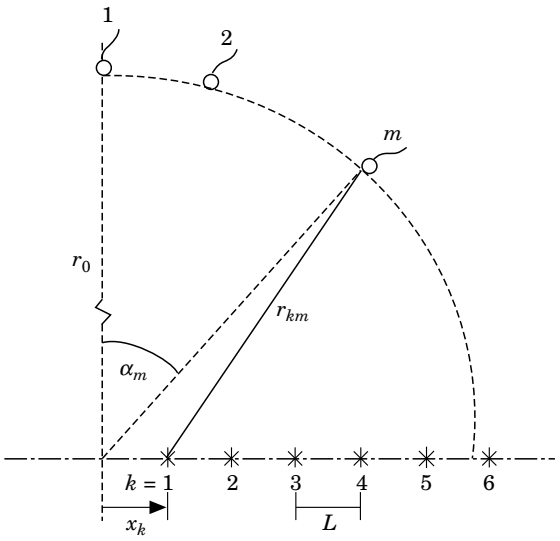

Figure 2. The model geometry.

and a geometric matrix H of dimensions $K^2 \times K^2$, where

$$H(p, q, k, l) \equiv \frac{1}{M} \sum_m \frac{1}{N} \sum_n \cos\left(\phi(m, n, k, l) - \phi(m, n, p, q)\right). \tag{2.7}$$

Hence, in matrix notation,

$$M = HB \tag{2.8}$$

and one is required to solve the inverse problem

$$B = H^{-1}M. \tag{2.9}$$

Hence it is immediately apparent that a crucial factor in obtaining satisfactory results is the condition and hence invertibility of the geometry matrix H. However, since this contains only geometric (and phase) information, its condition number can be employed, prior to any testing, to determine both the suitability of a proposed microphone array and to define frequencies for which results of uncertain accuracy may be obtained. We shall now proceed to explore these possibilities first analytically and subsequently via numerical simulation.

3. ANALYTICAL RESULTS

It is possible to make some progress in understanding the requirements for the successful inversion of equation (2.6) to obtain the required source parameters, (i.e., b_{kl}) via the idealized source model shown in Figure 2. Here the sources are all equally spaced at interval L such that $x_k = kL$, etc. The microphones are assumed to be located on a polar arc of large radius r_0 with the position of the mth microphone defined by the angle α_m, where $\sin \alpha_m = m \sin \Delta$: that is, the microphones are spaced by equal increments in the sine of the angle α. The approximations $r_{km} = r_0 - x_k \sin \alpha_m$ and $r_{ln} = r_0 - x_l \sin \alpha_n$ may then be invoked. Hence by inspection of equations (2.1) and (2.2) and using the definition of

$H(p, q, k, l)$ in equation (2.7) one finds

$$H(p, q, k, l) = \frac{1}{M}\sum_m \frac{1}{N}\sum_n \cos\left[\frac{\omega L \sin \Delta}{a_0}\{(k-p)m - (l-q)n\} - \frac{\omega L}{U_c}\{(k-p)-(l-q)\}\right]. \tag{3.1}$$

With an "appropriate" value of $\omega L \sin \Delta/a_0$, the oscillatory nature of the terms in this summation suggests that $H(p, q, k, l) = 1$ if $k = p$ *and* $l = q$, and $= 0$ otherwise. Inserting this result into equation (2.6) then yields the ideal result $\underline{\tilde{M}}(p, q) = b_{pq}$. Inspection of equation (2.5) shows that this result is entirely equivalent to having performed a discrete well resolved double Fourier transform on the data. This is expected, since Fourier transforms are well known as the equivalent of a least squares fit. We also note the implication from equation (3.1) that good quality results are likely to be obtained when the geometry matrix H has its principal values located on or close to the principal diagonal $k = p$, $l = q$. We shall now explore conditions under which this would not occur in the limits of high and low frequencies respectively.

3.1. HIGH FREQUENCY ALIASING

The occurrence of aliasing in equation (3.1) can be identified as a situation in which the argument of the cosine function increments by 2π for each term of the summation. The worse case, in the sense of the lowest frequency, can be identified by inspection as $l = q$ and $|k - p|$ obtaining its maximum possible value. However, since the product of the source spacing L and the maximum value of $|k - p|$ is just the total length of the source distribution, L_T say, then aliasing will potentially be present for all frequencies for which $\omega L_T \sin \Delta/a_0 \geqslant 2\pi$, or

$$f \geqslant a_0/(L_T \sin \Delta). \tag{3.2}$$

This is just the classical definition of an aliasing frequency, as given in references [1] and [2] for example, and corresponds to the phase of the cross-spectrum for a particular source changing by more than 2π between adjacent microphones.

In the present context, as we shall see below, it manifests itself by yielding finite values off the main diagonal of the geometric matrix, increasing its condition number and potentially yielding poor results at certain frequencies.

3.2. LOW FREQUENCY RESOLUTION

Inspection of equation (3.1) suggests that at low frequencies the variation of the argument of the cosine function may be too limited to yield the required cancellation when $k \neq p$ or $l \neq q$.

A quantitative description of this process is straightforward to obtain if one assumes that at such low frequencies the variation of the cosine function is sufficiently small between the discrete values so that the summation in equation (3.1) can be replaced by integrals in which m and n are treated as continuous variables. The result is

$$H(p, q, k, l) = \frac{\sin(\omega L \sin(\alpha_M/2)(k-p)/a_0)}{\omega L \sin(\alpha_M/2)(k-p)/a_0}\,\frac{\sin(\omega L \sin(\alpha_N/2)(l-q)/a_0)}{\omega L \sin(\alpha_N/2)(l-q)/a_0} \times \cos(\omega L/a_0)[(\sin(\alpha_M/2)-(1/M_c))(k-p)-(\sin(\alpha_N/2)-(1/M_c)(l-q))], \tag{3.3}$$

where $\sin \alpha_N = N \sin \Delta$ and $\sin \alpha_M = M \sin \Delta$. Hence the angles α_N and α_M define the aperture of the microphone array used in the summation over n and m respectively.

The nature of the geometric matrix $H(p, q, k, l)$ becomes clear if one rewrites equation (2.6) in the form

$$\tilde{M}(p, q) = \sum_k \sum_l b_{kl} H(p, q, k, l). \tag{3.4}$$

Inspection of equation (3.3) then suggests that, in the limit as the frequency tends to infinity, $H(p, q, k, l) = 1$ when $k = p$ *and* $l = q$, and $= 0$ otherwise, as a result of the sin X/X functions. Hence, as before, one finds that $\tilde{M}(p, q) = b_{pq}$.

However, at lower frequencies these sin X/X functions remain finite for finite values of either $k - p$ or $l - q$. They are the window functions associated with the finite aperture of the microphone array and remind us that under these circumstances contributions to the measurement vector $\tilde{M}(p, q)$ can arise from "sources" other than b_{pq}. However, the principal advantage of a parametric, as opposed to Fourier transform, method is that the matrix inversion, equation (3.4) or (2.9), allows for such contributions; it is fundamentally a deconvolution process. Hence, in principle, there is no low frequency limit below which results may not be obtained. However, in practice a lower frequency limit is set by the accuracy of the cross-spectral measurements and the resulting values of $\tilde{M}(p, q)$. We note from equation (3.3) that in the limit of low frequency all values of $H(p, q, k, l)$ tend towards unity, and the whoe matrix inversion becomes progressively more ill-conditioned and hence dependent on any errors in the measured values of $\tilde{M}(p, q)$.

4. THE INCOHERENT SOURCE ARRAY

The situation described above can be specialized to a set of incoherent sources by noting that, by definition,

$$b_{kl} \equiv a_k a_l c_{kl}, \tag{4.1}$$

so that for incoherent sources, where $c_{kl} = 1$ for $k = l$ and $= 0$ for $k \neq l$, equation (3.4) reduces to

$$\tilde{M}(p, p) = \sum_k b_k^2 H(p, p, k, k), \tag{4.2}$$

with, from equation (3.1),

$$H(p, p, k, k) = \frac{1}{M} \sum_m \frac{1}{N} \sum_n \cos\left[\frac{\omega L \sin \Delta}{a_0} (k - p)(m - n)\right].$$

In fact, this can be generalized by noting that kL is just the position of the kth source, x_k, and $m \sin \Delta$ is the angular position of the mth microphone, α_m. Hence equation (4.2) becomes

$$\tilde{M}(p, p) = \frac{1}{M} \sum_m \frac{1}{N} \sum_n \sum_k b_k^2 \cos \frac{\omega}{a_0} [(x_k - x_p)(\sin \alpha_m - \sin \alpha_n)].$$

This is the least squares fit expression of reference [2] for an incoherent source array, except that it contains a double, as opposed to single, summation over the microphones. Physically, this means that, while for the method given in reference [2] one measures only the cross-spectra between a single reference microphone and the other microphones in the

array, to evaluate the above expression one needs to measure the cross-spectra between all possible microphone combinations, each microphone in turn being used as the reference microphone. Inspection of the expression above indicates, however, that use of multiple reference microphones for the incoherent source case merely duplicates information, because the argument of the cosine function depends only on the microphone separation, i.e., $(\sin \alpha_m - \sin \alpha_n)$. Thus the benefits are probably marginal against the extra data processing effort involved, where for a 30-microphone array one would need to measure 900 as opposed to 30 cross-spectra. We note from the window function equation, equation (3.3), for example, that $H(p, p, k, k)$ is of the form $(\sin X/X)^2$, while for a single summation, equivalent to putting $\alpha_M = 0$, it becomes $\sin X/X$, only a marginal advantage in view of the deconvolution process described above.

We note, however, that the use of multiple reference microphones is *essential* for coherent sources. As inspection of equations (3.1) or (3.3) indicates, without the outer summation over m, equivalent to putting $m = 0$ in equation (3.1) and $\alpha_M = 0$ in equation (3.3), that one loses the ability to obtain low values of the window function when $l = q$, but $k \neq p$. This hopelessly ill-conditions the geometry matrix $H(p, q, k, l)$, because the results are basically ambiguous. Fortunately, as we shall proceed to demonstrate, via numerical simulation, only a selected few microphones of the total array need to be used as reference microphones.

5. THE INTERFERENCE TERMS

Before closing this section of analytical results, it is informative to identify two classes of terms inferred in the definition of the cross-spectra given in equation (2.2): i.e.,

$$C(m, n) = \sum_k \sum_l b_{kl} \exp \mathrm{j}\phi(m, n, k, l), \tag{5.1}$$

where $b_{kl} \equiv a_k a_l c_{kl}$.

The first group is comprised of those for which $k = l$ and their contribution to the cross-spectrum, $C_{k=l}(m, n)$, can be written for the far field microphone array as

$$C_{k=l}(m, n) = \sum_k a_k^2 \exp \mathrm{j}\left[\frac{\omega}{a_0}(\sin \alpha_n - \sin \alpha_m)x_k\right]. \tag{5.2}$$

In discrete form, this is the Fourier transform relationship of reference [1], and represents the form that the cross-spectrum would take if the sources were all mutually incoherent.

Some care is now necessary with the remaining terms, for which $k \neq l$. In deriving the least squares relationship in the Appendix it was implicitly assumed that b_{kl} and b_{lk} were independent variables. However, as their definition above makes clear, they are in fact identical. For interpretation purposes, therefore, it is useful to consider pairs of terms in equation (5.1) involving b_{kl} and b_{lk} respectively. Their sum is

$$S \equiv b_{kl} \exp \mathrm{j}\phi(m, n, k, l) + b_{lk} \exp \mathrm{j}\phi(m, n, l, k).$$

For a far field microphone array, this becomes

$$S = 2b_{kl} \cos \frac{\omega}{a_0} \left[(x_l - x_k) \left[\frac{\sin \alpha_n + \sin \alpha_m}{2} \right] + \frac{x_k - x_l}{M_c} \right]$$

$$\times \exp \mathrm{j} \frac{\omega}{a_0} \left[\frac{(x_l + x_k)}{2} (\sin \alpha_n - \sin \alpha_m) \right], \tag{5.3}$$

where $M_c = U_C/a_0$. Comparing equations (5.2) and (5.3) one sees that in the former the source position x_k is defined in the complex exponential term. A similar interpretation applied to equation (5.3) suggests that the "sources" of the interference terms are located at positions $(x_k + x_l)/2$. These "phantom" sources appear, therefore, at a position halfway between the actual sources. For equally spaced sources these may either occcupy positons between the actual sources or be superimposed on actual source positions. For example, the interference contribution from sources 2 and 4 will appear to be located at the position of source number 3, etc.

However, the important difference to be noted between equation (5.2) and equation (5.3) is that for the self-terms ($k = l$) in the former, the value of $C(m, n)$ depends only on the angular separation of the microphones, (i.e., $\sin \alpha_n - \sin \alpha_m$), not on their position. Conversely, equation (5.3) exhibits an additional directional feature through its cosine term, and it is this which permits one to separate the self- and cross-terms respectively, despite the fact that their "apparent positions" may be identical, as explained above.

6. NUMERICAL SIMULATION STUDIES

6.1. THE MODEL SIMULATION

The computer simulation model employed to support the work described above can be considered, roughly, to replicate shock cell noise generated by a 50 mm diameter nozzle operated with unheated air at a pressure ratio of order 3·0. Specifically, six shock cells are modelled as point monopoles, equally spaced at 50 mm intervals. The eddy convection velocity U_c was assumed to be 250 m/s. Each source is attributed unit source strength and the mutual coherence between source n and $n \pm 1$ is 0·75, that between n and $n \pm 2$ is 0·5, that between n and $n \pm 3$ is 0·25 and that between n and $n \pm 4$ and beyond is zero. The far field microphone array consists of a maximum of of 30 microphones situated around an arc of 10 m radius (200 nozzle diameters) centred on the nozzle outlet. The array covers the angular range 90° to 61° from the nozzle axis in 1° intervlas. The ambient speed of sound was taken as 342 m/s.

The simulations cover a frequency range from 1 kHz to 20 kHz at intervals of 100 Hz. For reference purposes we note that the principal peak shock associated noise frequency for the combination of source spacing and convection velocity specified above would range from 5 kHz at 90° to the nozzle axis to 7·9 kHz at 60°.

6.2. SIMULATION PROCEDURE

Equation (2.1) is used to generate a data file containing the cross-spectra between pairs of microphones. Each mircophone is paired with each other microphone giving, for the 30-microphone array, a total of 900 cross-spectra. This cross-spectra file is treated as a set of measured cross-spectra, from which estimates of the source strengths and coherences can be calculated using the methods described previously.

Unless otherwise stated, all matrix inversions are carried out by using L.U. decomposition with partial pivoting (based on reference [13]) and all calculations are to IEEE double precision. All program code (including matrix inversion routines) is written in BBC Basic VI and run on an Acorn Archimedes microcomputer.

6.3. STATISTICAL NOISE IN FAR FIELD CROSS-SPECTRA

In real measurement situations, the cross-spectra measured at the microphone array will be subject to a degree of statistical uncertainty. In order to simulate this uncertainty in the computer generated data, pre-specified amounts of equal probability random noise are added to the calculated cross-spectra. The noise error is defined relative to the sum of the mean squared source amplitudes at the array, i.e.,

$$\text{added noise} = \frac{e \times \text{rand}}{100} \sum_k \frac{a_k^2}{r_0^2},$$

where e is the specified percentage noise and "rand" is an equal probability number between -1 and $+1$. The noise is added to the real and imaginary parts of the cross-spectra prior to matrix generation. Note that the range of values that the added noise can take is proportional to $\pm e$, and that the statistical r.m.s. value of the noise is approximately proportional to e.

6.4. CALCULATION OF ERRORS

A measure of the performance of a particular microphone array and calculation procedure is obtained from the r.m.s. error between the calculated source strengths and coherence values (b'_{kl}) and those specified in the cross-spectral generation (b_{kl}). The resultant error is defined as

$$\text{r.m.s. error} = \left\{ \frac{1}{K^2} \sum_k \sum_l (b'_{kl} - b_{kl})^2 \right\}^{1/2},$$

where K is the number of sources. For the source distribution described above, the results can be considered to be acceptable if the r.m.s. error is less than 0·1. To demonstrate this, we present Figures 3(a) and 3(b) as a diagrammatic representation of a comparison between the actual source strengths and coherences and typically calculated values for r.m.s. errors of 0·05 and 0·5 respectively. The "T"-shaped symbols represent actual values and the "boxes" represent calculated values. One can see that, while the results of Figure 3(a) show an agreement of acceptable level for both source strength and coherence, with the higher r.m.s. error in Figure 3(b) significant differences of both source strength and particularly coherence values occur. Appraisal of a significant quantity of data of this type led to the conclusion that, for most purposes, an r.m.s. error of order 0·1 would be adequate.

In the remainder of this paper, the majority of results will be presented as the variation of this r.m.s. error with frequency. In view of the large range of vaues involved, a decibel scale, 20 $\log_{10}$ (r.m.s. error), is employed, with the desired value (0·1) shown as a horizontal line at -20 dB.

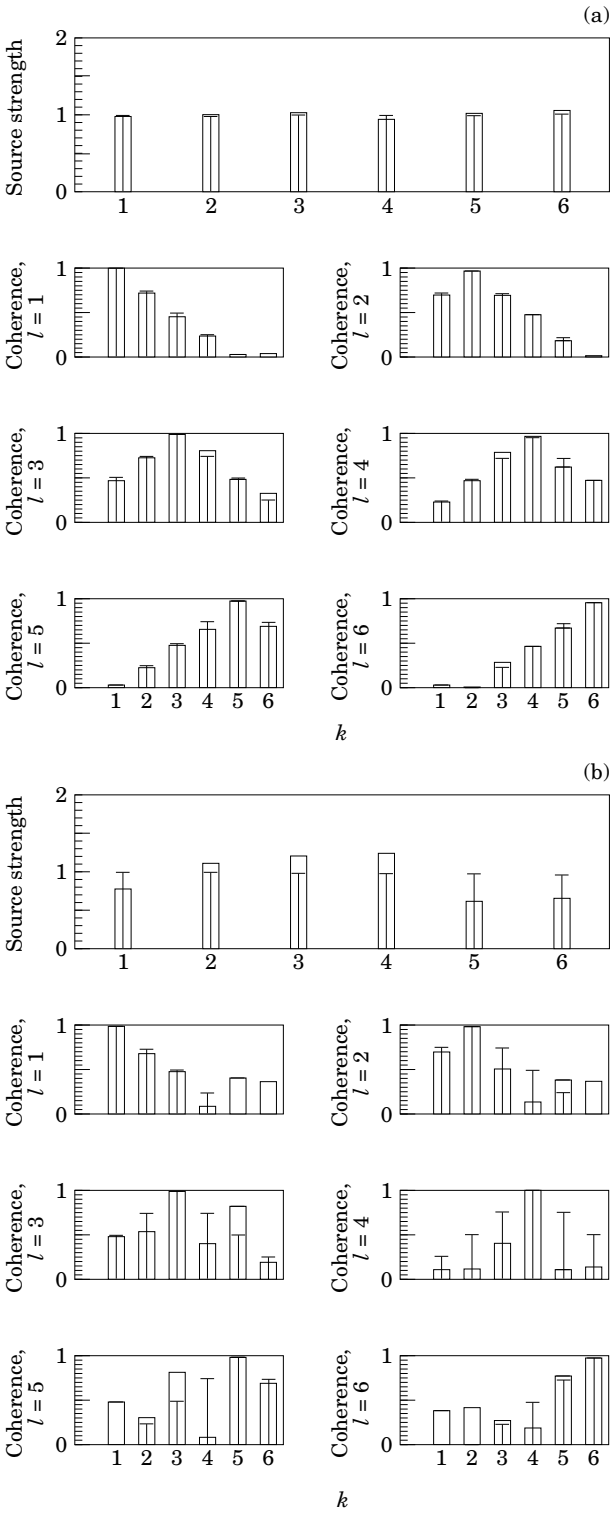

Figure 3. An example comparison between calculated and actual source strengths and coherences with an r.m.s. error in vector B of 0·05 (a) and 0·5 (b).

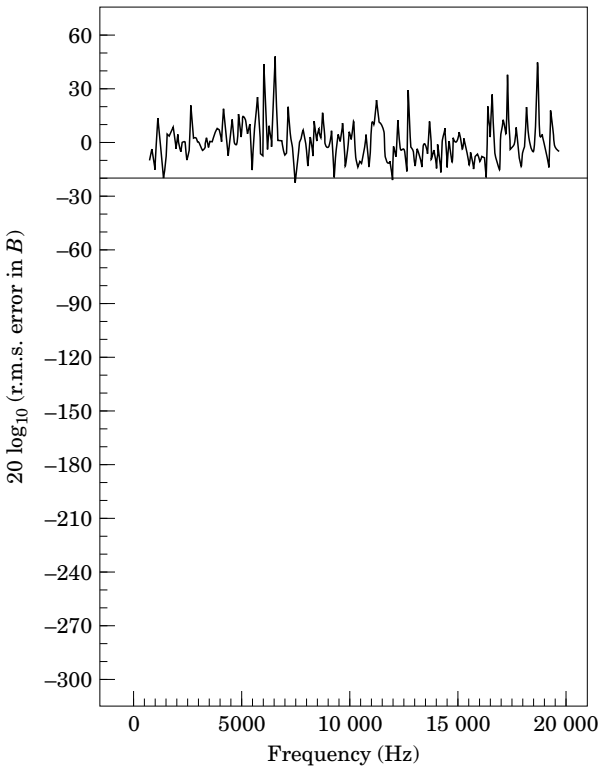

Figure 4. The r.m.s. error in vector B: 5×5 microphone array, least squares fit method, 0% error in far field data.

7. RESULTS OF NUMERICAL SIMULATION

7.1. NUMBER OF MICROPHONES REQUIRED

While, as described above, this simulation study was set up on the basis of 30 microphones covering a 30° arc the complete evaluation of, for example, equations (2.5) or (2.6) would require the calculation/measurement of 900 cross-spectra. From the practical viewpoint an important early consideration was therefore the determination of the minimum number of microphones which would yield satisfactory results over the specified frequency range. We note this is not specifically set in the "least squares" context, since "averaging" over the microphone array occurs prior to the formation of the matrices *per se*. It is the dimensions of the latter which are set by the source numbers, as outlined in section 2.1. However, guidance can be obtained on two grounds:

(a) As already noted, the required matrix inversion will be optimally conditioned when the principal values of the geometry matrix $H(p, q, k, l)$ are concentrated on or close to the main diagonal $k = p$, $l = q$. Inspection of the analytically derived window functions, equation (3.3), shows that the most rapid decay of these window functions will occur when the aperture angles α_M and α_N respectively are maximized. Hence the full 30° aperture should be employed.

(b) In the solution of any set of simultaneous equations, such as equation (2.2) for example, it is a fundamental requirement that there are at least as many knowns as unknowns. Hence, regardless of the method used, a minimum of six microphones are required to solve for six sources. However, for six incoherent sources the only unknowns

are their strengths, so that the measurement of the cross-spectra between a reference microphone and five others in the array is sufficient to yield six knowns and solve the problem; what is termed a 6×1 array is adequate. However, for six partially coherent sources there are a total 36 unknowns. Here the 36 "knowns" can be generated with six microphones by using each microphone in the array successively as the reference; the so-called 6×6 array.

Evidence that this is indeed the case can be seen by comparison of Figures 4 and 5. In the former, a 5×5 microphone array was employed for our model of six partially coherent sources. Even with zero error, apart from computer rounding errors, in the far field data, the r.m.s. error in the results is large over the entire frequency range. In marked contrast, use of a 6×6 array, as shown in Figure 5, yields excellent results at all frequencies for perfect input data. With 5% statistical error superimposed on the far field cross-spectra, the results are satisfactory above about 7 kHz, based on the -20 dB criterion, except for two isolated regions around 13 and 17 kHz respectively.

The identification of the origin of these latter regions of poorer results is straightforward. Choosing to use a minimum number of microphones, six, but to spread them over the full 30° arc to maximize low frequency resolution, has created a spacing between adjacent microphones of 6°. Reference to the approximate expression for $H(p, q, k, l)$ in equation (3.1) and the condition for aliasing given in expression (3.2) shows that for this microphone separation aliasing, and hence potentially large values for $H(p, q, k, l)$ for $k \neq p$ and $l \neq q$ can now occur for any frequency above 13 kHz. Hence, for frequencies above 13 kHz, a closer microphone spacing is required.

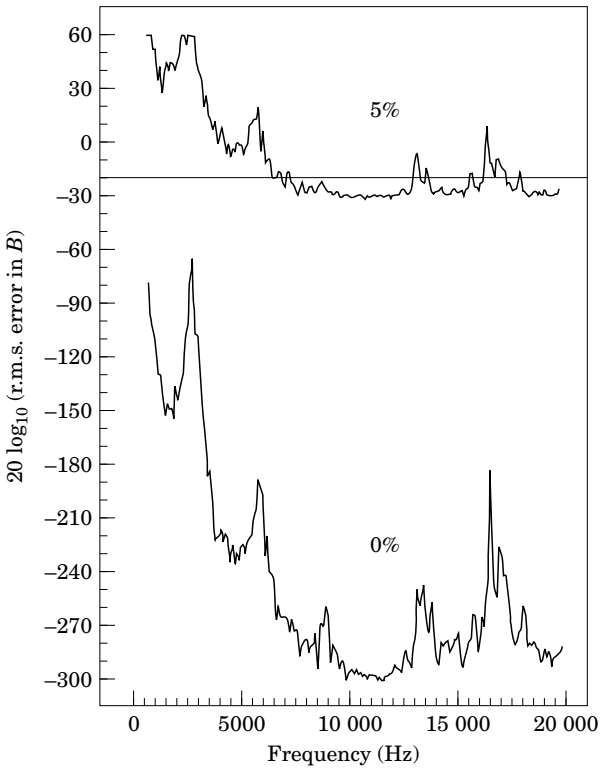

Figure 5. The r.m.s. error in vector B: 6×6 microphone array, least squares fit method, 0% and 5% error in far field data.

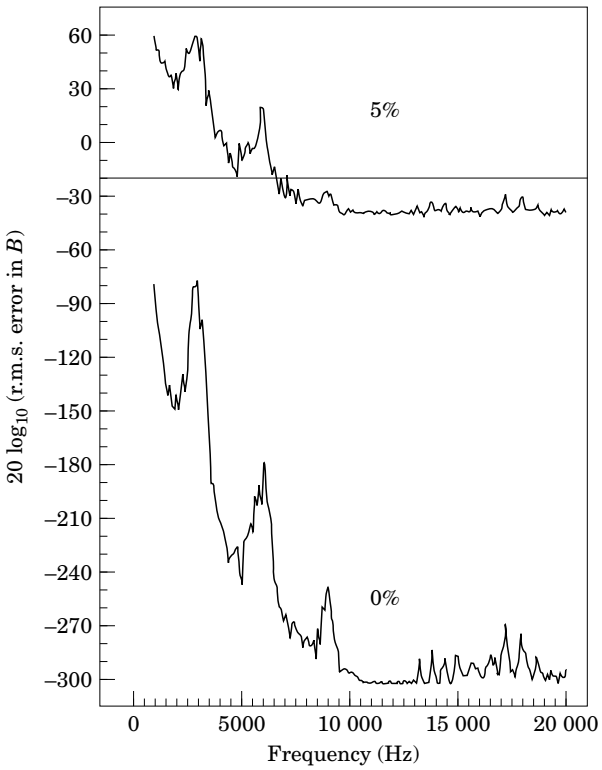

Figure 6. The r.m.s. error in vector B: 30×6 microphone array, least squares fit method, 0% and 5% error in far field data.

While, in principle, there are several straightforward ways of achieving this—for example, 7×7 array at 4° spacing would be almost adequate up to 20 kHz—there are other practical requirements to be considered. First, from a data processing viewpoint it is advantageous to keep the number of reference microphones to a minimum. Second, in designing an array for practical use it is always undesirable to work on the limits of the aliasing criteria. Any unexpected source outside the anticipated source distribution can then invalidate the complete data set acquired.

These considerations led to the idea of testing a 30×6 array. That is, the complete set of 30 microphones is employed, but with the number of reference microphones held at the minimum of six. In terms of equation (3.1) for $H(p, q, k, l)$, this is equivalent to reducing $\sin \Delta \approx \Delta$ to 1° and incrementing the value n in steps of unity. The value of m is, however, incremented in steps of six. Hence aliasing effects in respect of finite values of $l - q$ are entirely eliminated; they are restricted to a few values of $k - p$, but only when $l = q$.

The results obtained by using this procedure are shown in Figure 6. Evidence of some weak residual aliasing effects is apparent in the r.m.s. error variations above 13 kHz, particularly for the case of the perfect far field data. However, these effects are relatively weak, and even for 5% error in the cross-spectral data all results above about 7 kHz conform to the -20 dB error criterion.

Finally in this context, we turn to the results obtained by using the full 30×30 array, which are shown in Figure 7. The unsteadiness in the, albeit small, errors above 13 kHz seen in Figure 6 has now disappeared, indicating that this array has now eliminated all aliasing effects. The only other difference is some reduction in r.m.s. error for the results

obtained from data with 5% statistical error in the cross spectra. In fact, inspection of Figures 5, 6 and 7, corresponding to 6×6, 30×6 and 30×30 arrays respectively, indicates that, as we might expect, there has been a progressive improvement above 10 kHz as the number of degrees of freedom in the least squares fit procedure has increased. However, whether the improvement between Figures 6 and 7 is worthwhile in view of the extra data processing involved is considered to be debatable.

7.2. THE LOWER FREQUENCY BEHAVIOUR

In contrast to the variation and general improvement of results obtained amongst Figures 5, 6 and 7 for the higher frequencies, the results below about 10 kHz show very little dependence on the microphone array employed. In all cases the r.m.s. errors show a general, fairly rapid, increase as the frequency reduces below 10 kHz, with a sinusoidal variation modulating this increase. The former had been anticipated on the basis of the analytical window functions given in equation (3.3). For the case of the equal aperture angles $\alpha_N = \alpha_M$, these can be written as

$$H(p, q, k, l) = \frac{\sin (k-p)X}{(k-p)X} \times \frac{\sin (l-q)X}{(l-q)X} \times \cos \frac{\omega L}{a_0} \left\{ \left(\sin \frac{\alpha_M}{2} - \frac{1}{M_c} \right) ((k-p)-(l-q)) \right\}, \tag{7.1}$$

where $X \equiv (\omega L/a_0) \sin (\alpha_M/2)$. As discussed previously, therefore, at the higher frequencies it is the terms $\sin (k-p)X/(k-p)X$ which ensure that the major terms in the geometric

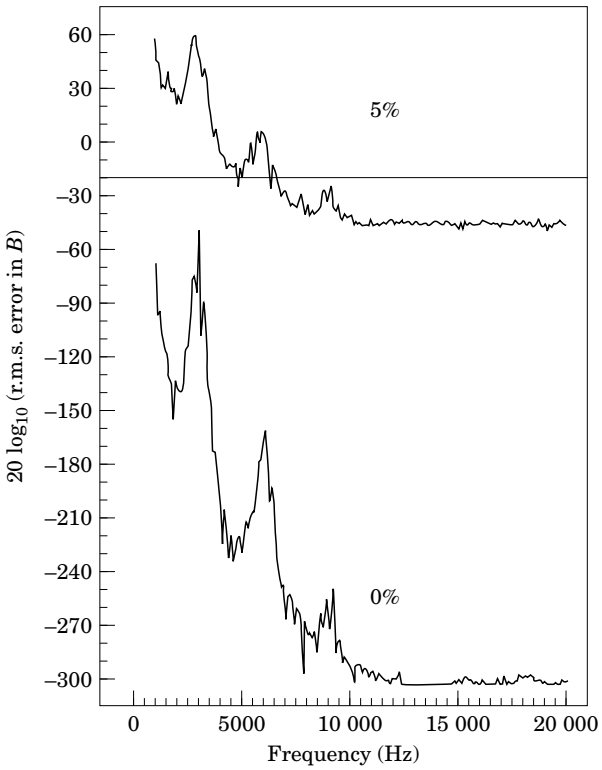

Figure 7. The r.m.s. error in vector B: 30×30 microphone array, least squares fit method, 0% and 5% error in far field data.

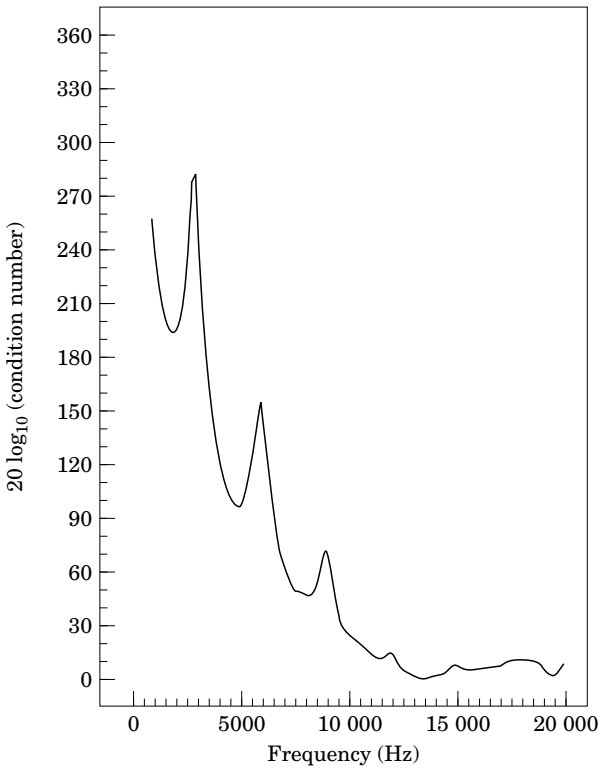

Figure 8. The condition number of matrix H: 30×30 microphone array

matrix are concentrated around its main diagonal $k = p$ *and* $l = q$. However, as the frequency reduces, these functions obtain significant values for finite values of $k - p$ or $l - q$. Using as an arbitrary criterion that these functions should be reduced to their first zero when $|k - p|$ or $|l - q|$ equals one, yields the condition $f \geqslant a_0/[2L \sin(\alpha_M/2)]$, which, for the current model, yields $f \geqslant 13{\cdot}2$ kHz.

One might anticipate, therefore, a progressive deterioration in the condition of the geometric matrix below this frequency, as the off-diagonal terms progressively increase their values. This effect is shown in Figure 8 for the 30×30 array. Perhaps even more remarkable, however, is the way in which the variation of the contidion number mirrors the increasing, but cyclic, behaviour of the r.m.s. errors for this array shown previously in Figure 7. Furthermore, while a general increase in condition number and r.m.s. error had been anticipated on the basis of the increasing $\sin Z/Z$ functions discussed above, the cyclic behaviour had not. In fact, at first sight the results presented in Figures 7 and 8 might suggest that certian "critical" or "problem" frequencies exist for the least squares fit method which, for the current model, occur at approximately 3, 6 and 9 kHz.

This prompted a search for alternative methods of inversion which might avoid these apparent difficulties. In Figure 9, for example, is shown the result of the direct, forced fit, inversion of equation (2.2) using the required 6×6 array. In comparison with the equivalent least squares data, shown in Figure 5, one can note that (a) the effect of aliasing is far more apparent and leads to much larger errors at the higher frequencies when direct inversion is employed, and (b) while the cyclic behaviour of the r.m.s. errors at frequencies below 10 kHz has now been eliminated, the error curve passes through the peaks of the error curve for the least squares method, as shown in Figure 5.

Somewhat similar results were obtained by using Singular Value Decomposition in conjunction with the more practical 30×6 microphone array. The results are shown in Figure 10, and may be compared with the equivalent least squares data shown in Figure 6. One can observe that (a) the increase in error due to aliasing at 13 and 17 kHz, which had been virtually eliminated for the least squares data in Figure 6, is now clearly apparent in Figure 10, and (b) while the cyclic behaviour of the error curve is absent at low frequencies, it again passes through the peaks of the error curve in Figure 6.

Hence we conclude that the proposed least squares method actually outperforms these alternatives at both high and low frequencies.

As to the cyclic behaviour problem, the clue to this lies in equation (7.1). One can observe that the cyclic behaviour is associated with that frequency range in which the $\sin Z/Z$ functions do not necessarily obtain small values for finite values of $k - p$ and $l - q$. However, the actual value of $H(p, q, k, l)$ also depends on the cosine function. Hence while the values of the $\sin Z/Z$ functions may not be particularly small, a significant number of the values of $H(p, q, k, l)$ may be as a result of low values of this associated cosine function and hence the matrix condition number is reduced.

The exceptions, in fact, occur when the argument of this cosine function is an integer multiple of π for all values of $k - p$ and $l - q$, thus guaranteeing the maximum magnitude of $H(p, q, k, l)$ everywhere. Inspection of equation (7.1) shows that this occurs at the

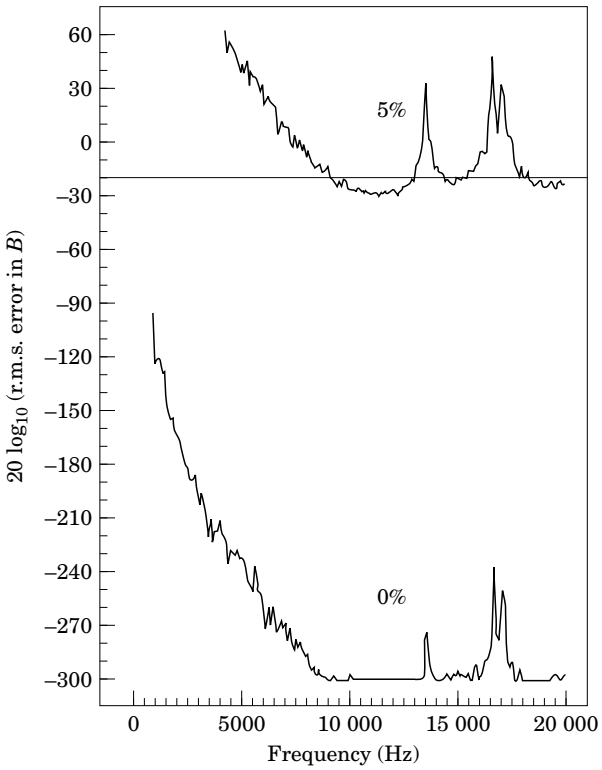

Figure 9. The r.m.s. error in vector B: 6×6 microphone array, direct inversion method, 0% and 5% error in far field data.

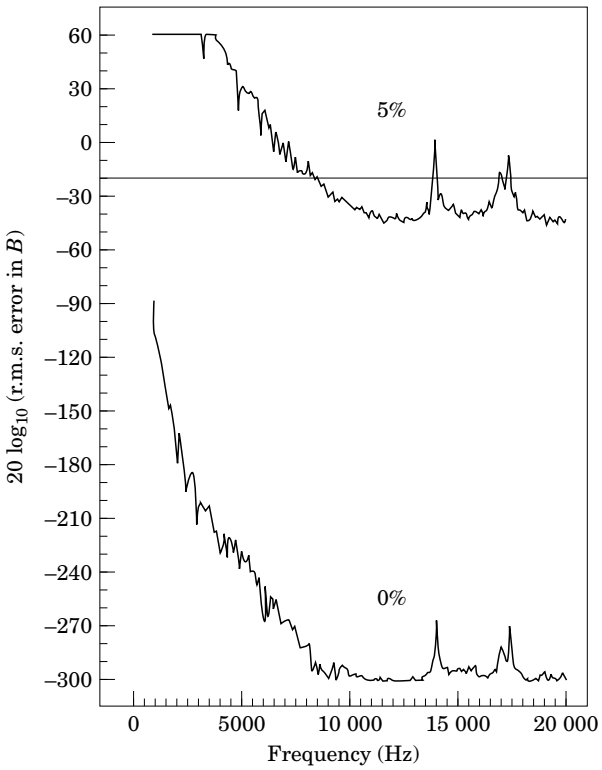

Figure 10. The r.m.s. error in vector B: 30 × 6 microphone array, singular value decompositon, 0% and 5% error in far field data.

frequency

$$f = \frac{a_0}{2L}\left|\sin\frac{\alpha_m}{2} - \frac{1}{M_c}\right|^{-1},$$

and harmonics thereof. Evaluating these frequencies for the current model yields 3·08, 6·16 and 9·24 kHz, in precise agreement with the peaks in the condition number variation shown in Figure 8. However, between these peaks the condition number is lower for certain frequency ranges and hence more accurate results can be obtained. In Figures 6 and 7, for example, it is indicated that, on the basis of our -20 dB criterion, just adequate results can be obtained at 5 kHz, although those at 6 kHz would not be acceptable. The fact that these frequencies can be determined from the variation of the condition number of the geometry matrix, prior to any testing, and to some extent controlled by choice of the microphone aperture, $\sin(\alpha_M/2)$, is considered to be a valuable feature of the present procedure.

8. CONCLUSIONS

(1) The principal objective of the work presented in this paper has been to explore the feasibility and limitations of a proposed least squares fit method for the determination of the amplitudes and mutual coherence of a set of monopole sources. It constitutes the next

logical step from the work of reference [2] to the extent that the restriction to incoherent sources has been removed.

(2) Although the model considered here has been restricted to a line source array, as explained in section 2 the basic requirement is a knowledge of the positions and relative phasing of the constituent sources. While this has been convenient as an intermediate step, the next logical advance is to remove the requirement for known phasing, and this development is currently under investigation at the ISVR by Yoon and Nelson [14].

(3) The heart of the present system is described by equation (2.5) which can be written in matrix form as $M = HB$, where M is the measurement vector, H a geometric matrix and B the required vector of source strengths and coherences as described previously. The required solution is therefore $B = H^{-1}M$. An essential feature of the procedure is therefore the condition number and hence invertibility of this geometry matrix. A powerful feature of the current procedure is that this condition number, specifically its variation with frequency, can be determined prior to any testing and hence used to aid the design of a microphone array and/or determine that range of frequencies over which satisfactory results may be obtained.

(4) Subject to the general condition that the number of microphones must equal or exceed the number of sources, factors which will adversely effect the condition number of this geometric matrix and lead to poor quality results are the following: (a) an inadequate microphone array aperture leading, physically, to a lack of resolution at lower frequencies; (b) an excessive spacing between microphones which leads to aliasing effects. Both effects are clearly shown in the condition number of the geometry matrix irrespective of the complexity of either the source or microphone array geometry.

(5) However, in terms of our simple line source array with equal source spacing, L, both the analytical and numerical simulation results indicate the following. (a) At low frequencies the condition number will begin to increase when the $\sin Z/Z$ functions in equation (3.3) or (7.1) do not reach their first zero for $|k-p|$ or $|l-q|$ equal to unity; on this criterion one needs

$$f \geqslant a_0/[2L \sin(\alpha_m/2)]. \tag{8.1}$$

However, the rate of increase is relatively slow for about an octave below this frequency so that, as discussed below, for reasonable levels of statistical error in the cross-spectral data one might expect acceptable results down to about half this frequency.

(b) As specified in section 3.1, aliasing will begin to occur when the frequency exceeds

$$f \geqslant a_0/(L_T \sin \Delta), \tag{8.2}$$

where L_T is the total length of the source distribution and Δ is the microphone spacing. It is to satisfy this criterion (see equation (3.1)) which leads to the need for the use of multiple reference microphones in conjunction with coherent sources. Strictly, one needs to satisfy the criterion (8.2) for the highest frequency of interest. However, as discussed in section 7.1, there are practical advantages in utilizing a small spacing for the main array and then selecting the minimum number of these microphones for use as reference microphones. This led to the adoption of the 30×6 array in the present simulation study of six sources. This allows a large safety margin against aliasing created by unsuspected sources of noise outside the anticipated source array, as well as building extra degrees of freedom into the least squares fit, which serves to reduce the r.m.s. error of the results.

(c) We shall finally consider the relationship between the condition number of the geometry matrix, statistical error in the cross-spectral data and the quality of the source strength and coherence results. The first point to note is that it is completely non-productive to examine the potential of techniques of this nature on the assumption

that the cross-spectral data is entirely accurate. Had this been done in the present study, one would have concluded that high precision results would be obtained at all frequencies examined $1 \leqslant f \leqslant 20$ kHz with all the microphone arrays tested, with the single exception of the clearly inadequate 5×5 array.

The results indicate, in fact, that the following factors all play their part in determining the r.m.s. error of the final results and the frequency range over which adequate results may be obtained: the condition number of the geometry matrix; the statistical error in the far field cross-spectral data; the number of cross-spectra used in the least squares fit procedure. Of these, the former two are the more important parameters at low frequencies, with the results indicating that for 5% error in the cross-spectral data a condition number of about 10^5 or less is required to achieve our proposed criterion of 0·1 r.m.s. error (i.e., the -20 dB error criterion).

We note finally that while, as specified in section 6.2, the majority of the simulations reported here were carried out by using IEEE double precision, some additional work, not included here indicates that this is completely unnecessary whenever realistic amounts of statistical error are present in the cross-spectral data.

ACKNOWLEDGMENTS

The authors wish to express their appreciation to the following people: to Mr R. A. Pinker and the staff of the Noise Section at the Defence Research Agency, Pyestock, for both their technical and financial support for this work; to members of the Rolls Royce Noise Department, particularly Dr A. Kempton, Mr W. Boyd, Mr P. Strange and Mr M. Chamberlain, for their interest and encouragement. One of us (M.J.F.) also wishes to acknowledge the financial support provided by Rolls Royce plc.

REFERENCES

1. M. J. Fisher, M. Harper-Bourne and S. A. L. Glegg 1977 *Journal of Sound and Vibration* **51**, 23–54. Jet engine source location: the polar correlation technique.
2. B. J. Tester and M. J. Fisher 1981 *Proceedings of AIAA 7th Aero-Acoustics Conference*, *AIAA Paper No*. 81-2040. Engine noise source breakdown: theory, simulation and results.
3. M. Harper-Bourne and M. J. Fisher 1973 *Proceedings of AGARD Conference* (*Preprint No*. 131) *on Noise Mechanisms*, *Brussels*. The noise from shock waves in supersonic jets.
4. T. E. Siddon 1971 *Proceedings of the 7th International Congress on Acoustics*, *Budapest*, 533–563. New correlation method for the study of flow noise.
5. W. T. Chu, J. Laufer and K. Kao 1972 *International Conference on Noise Control*, *Washington*, *D.C*., 472–476. Noise source distribution in subsonic jets.
6. F. R. Grosche 1973 *AGARD Conference CP* 131 *on Noise Mechanisms*. Distributions of sound source intensities in subsonic jets.
7. S. Glegg 1975 *M.Sc*. *Dissertation*, *University of Southampton*. Jet noise source location using an acoustic mirror.
8. J. Billingsley and R. Kinns 1976 *Journal of Sound and Vibration* **48**, 485–510. The acoustic telescope.
9. M. Mosher 1996 *AIAA Paper* 96-1713. Phased arrays for aeroacoustic testing: theorectical development.
10. S. A. Glegg *et al*. 1979 *Ph.D*. *Dissertation*, *University of Southampton*. Jet noise source location.
11. P. J. R. Strange 1984 *AIAA Paper No*. 84-2361. Coaxial jet noise source distribution.
12. A. J. Kempton 1976 *Journal of Sound and Vibration* **48**, 475–483. The ambiguity of acoustic sources—a possibility for active control?
13. W. H. Press *et al*. *Numerical Recipes in Fortran*. Cambridge: Cambridge University Press.
14. S. H. Yoon and P. A. Nelson 1996 *Proceedings of Internoise* 96, *Liverpool*, **6**, 3021–3026. Least squares technique for the estimation of acoustic source strength spectra.

APPENDIX

A.1. THE LEAST SQUARES FIT

The relationship between the cross-spectrum of microphones m and n and the required set of source amplitudes and coherences b_{kl} is

$$C(m, n) = \sum_k \sum_l b_{kl} \exp \mathrm{j}\phi(m, n, k, l). \tag{A1}$$

We now wish to identify a set of source parameters, b_{pq} say, which will minimize the mean square error between a set of cross-spectral measurements $\tilde{C}(m, n)$ and the model given by equation (A1).

Let this mean square error σ^2 be

$$\sigma^2 \equiv \sum_{mn} |\tilde{C}(m, n) - C(m, n)|^2, \tag{A2}$$

where, for this Appendix only,

$$\sum_{mn} \equiv \frac{1}{m} \sum_m \frac{1}{N} \sum_n .$$

Upon writing $\tilde{C}(m, n)$ and $C(m, n)$ in terms of their real and imaginary parts equation (A2) becomes

$$\sigma^2 = \sum_{mn} (\tilde{R}(m, n) - R(m, n))^2 + (\tilde{I}(m, n) - I(m, n))^2.$$

Hence the requirement that the mean square error is a minimum, i.e., $\partial\sigma^2/\partial b_{pq} = 0$, leads to

$$\sum_{mn} (\tilde{R}(m, n) - R(m, n)) \frac{\partial R(m, n)}{\partial b_{pq}} = -\sum_{mn} (\tilde{I}(m, n) - I(m, n)) \frac{\partial I(m, n)}{\partial b_{pq}} ,$$

which can be rearranged as

$$\sum_{mn} \tilde{R}(m, n) \frac{\partial R(m, n)}{\partial b_{pq}} + \tilde{I}(m, n) \frac{\partial I(m, n)}{\partial b_{pq}} = \sum_{mn} R(m, n) \frac{\partial R(m, n)}{\partial b_{pq}} + I(m, n) \frac{\partial I(m, n)}{\partial b_{pq}} . \tag{A3}$$

In the present formulation in which the phasing of the sources are assumed known and are contained in the phase angle $\phi(m, n, k, l)$, it follows that the values of b_{kl} are purely real. Hence

$$R(m, n) = \sum_k \sum_l b_{kl} \cos \phi(m, n, k, l), \qquad I(m, n) = \sum_k \sum_l b_{kl} \sin \phi(m, n, k, l), \tag{A4}$$

and hence

$$\frac{\partial R(m, n)}{\partial b_{pq}} = \cos (m, n, p, q), \qquad \frac{\partial I(m, n)}{\partial b_{pq}} = \sin (m, n, p, q), \tag{A5}$$

Inserting these relationships into equation (A3) then yields

$$\sum_{mn} \tilde{R}(m, n) \cos \phi(m, n, p, q) + \tilde{I}(m, n) \sin \phi(m, n, p, q)$$

$$= \sum_{m\,n} \sum_{k} \sum_{l} b_{kl} \cos (\phi(m, n, k, l) - \phi(m, n, p, q)), \tag{A6}$$

which is the result quoted as equation (2.5).

A.2. THE NATURE OF THE MINIMUM

Using the expression for σ^2 given above, one finds that

$$\frac{\partial \sigma^2}{\partial b_{pq}} = \sum_{mn} -2 \left[(\tilde{R}(m, n) - R(m, n)) \frac{\partial R(m, n)}{\partial b_{pq}} + (\tilde{I}(m, n) - I(m, n)) \frac{\partial I(m, n)}{\partial b_{pq}} \right]$$

and hence

$$\frac{\partial^2 \sigma^2}{\partial b_{pq}^2} = 2 \sum_{mn} \left(\frac{\partial R(m, n)}{\partial b_{pq}} \right)^2 + R(m, n) \frac{\partial^2 R(m, n)}{\partial b_{pq}^2}$$

$$- \tilde{R}(m, n) \frac{\partial^2 R(m, n)}{\partial b_{pq}^2} + \left(\frac{\partial I(m, n)}{\partial b_{pq}} \right)^2 + I(m, n) \frac{\partial^2 I_{mn}}{\partial b_{pq}^2} - \tilde{I}(m, n) \frac{\partial^2 I(m, n)}{\partial b_{pq}^2}.$$

Inserting the expressions for these terms from equations (A4) and (A5) and noting from the latter $\partial^2 R(m, n)/\partial b_{pq}^2 = 0$ and $\partial^2 I(m, n)/\partial b_{pq}^2 = 0$, one finds that

$$\frac{\partial \sigma^2}{\partial b_{pq}^2} = 2 \sum_{mn} \{\cos^2 (m, n, p, q) + \sin^2 (m, n, p, q)\} = 2.$$

Since 2 is positve, this shows there are no maxima and therefore only one single minimum.